JAERI - M
89-086

RIPPLE LOSS OF ALPHA PARTICLES IN ITER

July 1989

Keiji TANI, Tomonori TAKIZUKA and Masafumi AZMI

日 本 原 子 力 研 究 所
Japan Atomic Energy Research Institute

JAERI-Mレポートは，日本原子力研究所が不定期に公刊している研究報告書です。
入手の問合わせは，日本原子力研究所技術情報部情報資料課（〒319-11茨城県那珂郡東海村）あて，お申しこしください。なお，このほかに財団法人原子力弘済会資料センター（〒319-11 茨城県那珂郡東海村日本原子力研究所内）で複写による実費領布をおこなっております。

JAERI-M reports are issued irregularly.
Inquiries about availability of the reports should be addressed to Information Division, Department of Technical Information, Japan Atomic Energy Research Institute, Tokai-mura, Naka-gun, Ibaraki-ken 319-11, Japan.

編集兼発行　日本原子力研究所
印　　刷　㈱原子力資料サービス

JAERI-M 89-086

Ripple Loss of Alpha Particles in ITER

Keiji TANI, Tomonori TAKIZUKA[+] and Masafumi AZUMI

Department of Large Tokamak Research
Naka Fusion Research Establishment
Japan Atomic Energy Research Institute
Naka-machi, Naka-gun, Ibaraki-ken

(Received June 13, 1989)

Part I: A benchmark test for the ripple loss of alpha particles in ITER has been executed by using an orbit-following Monte-Carlo (OFMC) code. In ITER with a plasma current of the order of 10 MA and an edge ripple of the order of 3%, the total power-loss fraction derived by JAERI's OFMC code is 6.6%.

Part II: Two dimensional heat load on the first wall due to ripple loss of alpha particles in ITER has been estimated by using an OFMC code. The peak heat load due to ripple-trapped loss is of the order of 0.1 MW/m^2. The peak heat load by ripple-untrapped loss averaged over the toroidal angle is about 0.07 MW/m^2.

Keywords: Alpha particle, Ripple loss, Benchmark test, Heat load, ITER

+ Department of Thermonuclear Fusion Research

JAERI－M 89－086

ITERにおけるアルファ粒子のリップル損失

日本原子力研究所那珂研究所臨界プラズマ研究部
谷　　啓二・滝塚　知典[+]・安積　正史

（1989年6月13日受理）

第Ⅰ部：ITERにおけるα粒子のリップル損失に関するベンチマークテストを軌道追跡モンテカルロ（OFMC）コードを用いて行なった。ITERでは，プラズマ電流が10MA程度，プラズマのトーラス外周端でのリップル率が3％の条件で，α粒子のパワー損失比6.6％が原研のOFMCコードで得られた。

第Ⅱ部：ITERにおけるα粒子のリップル損失による真空容器第1壁上の2次元的熱負荷分布を軌道追跡モンテカルロコードを用いて求めた。リップル捕捉損失粒子によるピーク熱負荷は約0.1MW／m^2。リップル非捕捉損失粒子による熱負荷のトロイダル角平均値の最大は約0.07MW／m^2。

那珂研究所：〒311－01　茨城県那珂郡那珂町大字向山801－1
＋核融合研究部

Contents

目　　次

Preface

This report summarizes the results of numerical evaluation of ripple losses of alpha particles in ITER which were presented in the specialist meeting held in Garching, March 8-10, 1989. The report consists of two parts; in the first, the results of benchmark test of OFMC code are presented for a model ITER configuration and, in the second part, the two dimensional profile of the alpha-particle ripple losses on the first wall is investigated in detail.

The authors would like to express their sincere thanks to Dr. T. Tsunematsu for the useful discussions and his continued effort to arrange the specialist meeting. The authors are also grateful to Drs. S. Mori, K. Tomabechi, M. Yoshikawa and S. Tamura for their continuous encouragements.

I. Benchmark Test for Ripple Loss of Alpha Particles in ITER

1. Introduction

There are several numerical codes with different calculation models to evaluate the ripple losses of alpha particles. In order to make a cross-check of those codes and to resolve possible discrepancies among them due to the differences in the numerical algorithms, a benchmark test has been proposed.

In a plasma with very low I_p and/or very high field ripple, the loss fraction approximates to about $\varepsilon^{1/2}$ since most of the banana-trapped particles escape from the plasma [1]. Then, it might be very difficult to find the significant differences in the numerical results from those codes. On the other hand, in a plasma with very high I_p and/or very low field ripple, the loss fraction becomes very small, so that the Monte-Carlo error bar becomes very large. Accordingly, we propose a benchmark calculation with parameters which may give a ripple-loss fraction of the order of $(1/2 \sim 1/4)\varepsilon^{1/2}$

2. Calculation parameters

Calculation parameters are summarized in Table 1. The preliminary investigations on the ripple losses of alpha particles in ITER indicate very low ripple loss fractions [2]. Therefore, we employed a rather lower plasma current ($I_p = 10\,MA$) and a higher edge field ripple ($\delta_0 = 3\,\%$). Geometry of MHD equilibrium and constant contours of field ripple are shown in Fig.1. For the simplicity of calculation, we consider a simple rectangular first wall which is also shown in Fig.1. Distributions of the field ripple and the toroidal flux function ψ in the midplane are plotted in Fig.2. The safety factor q is shown in Fig.3 as a function of ψ.

3. Calculation results

Calculation has been made by using an orbit-following Monte-Carlo code. The characteristics of our code are summarized in Table 2

The evolution of the time-integrated total power-loss fraction G_t is shown by the solid curve in Fig.4. For reference, the time-accumulated power-loss fraction of ripple-trapped loss G_{rt} is also shown in Fig.4 by the dotted curve (red region). The power-loss fraction of ripple-enhanced banana-drift (ripple-untrapped) loss G_{bd} is given by the difference between those two curves (blue region). Finally, at $t = \tau_s$, where τ_s is the slowing

down time at the plasma center, $G_{rt}=3.4\%$, $G_{bd}=3.2\%$ and $G_t=6.6\%$ are estimated.

The evolution of the time-integrated total particle-loss fraction F_t, the sum of the particle fractions of ripple-trapped loss F_{rt} and banana-drift loss F_{bd}, is shown in Fig.5 by the solid curve. The time evolution of F_{rt} is also shown in Fig.2 by the dotted curve. At $t=\tau_s$, $F_{rt}=11.9\%$, $F_{bd}=4.4\%$ and $F_t=16.3\%$ are obtained. In the present case the ripple-trapping is very important as a loss mechanism.

The energy spectrum of loss particles is another important measure for the benchmark test of this sort of problem. Accordingly, the energy spectrum of ripple-enhanced banana-drift loss particles $S_{bd}(E)$ is diagnosed and is shown in Fig.6 by the blue poles. The spectrum of ripple-trapped loss particles $S_{rt}(E)$ is also shown in Fig.6 by the red poles. The spectrum S_{bd} has a very sharp peak near the birth energy. On the other hand, S_{rt} shows a dull peak in the low energy region.

Fractions of alpha power deposited to bulk plasma electrons, deuterons, tritiums and impurity ions are 72%, 11%, 8% and 1.6%, respectively.

4. Conclusions

A benchmark test for the ripple loss of alpha particles in ITER has been executed by using an orbit-following Monte-Carlo (OFMC) code. In ITER with a plasma current of the order of 10 *MA* and an edge ripple of the order of 3%, the total power- and particle-loss fractions derived by JAERI's OFMC code are 6.6% and 16.3%, respectively. In the present case the ripple-trapping is very important as a loss mechanism.

References

[1] TANI, K., TAKIZUKA, T., AZUMI, M., KISHIMOTO, H., Nucl. Fusion 23 (1983) 657.

[2] TAKIZUKA, T., TANI, K., AZUMI, M., "ITER Specialist Meeting on Confinement" May 24-27 1988.

Table 1 Calculation parameters

major radius	$R_t = 5.8\ m$
minor radius	$a = 2.2\ m$
toroidal field	$B_t = 4.4\ T$
plasma temperature	$T_e(\Psi) = T_{e0}(1-\Psi)$
	$T_i(\Psi) = T_{i0}(1-\Psi)$
	$T_D(\Psi) = T_T(\Psi) = T_i(\Psi)$
	$T_{e0} = T_{i0} = 20\ keV$
plasma density	$n_e(\Psi) = n_{e0}(1-\Psi)^{0.5}$
	$n_D(\Psi) = n_T(\Psi) = n_i(\Psi)$
	$n_{e0} = 2.0 \times 10^{20}\ m^{-3}$
plasma current	$j(\Psi) = j_0(1-\Psi)^{0.5}$
	$I_p = 10\ MA$
ellipticity	$\kappa = 1.96$
triangularity	$\Delta = 0.55$
effective Z	$Z_{eff} = 1.5$ (uniform)
charge number of impurity ion	$Z_{imp} = 8.0$ (oxygen)
number of toroidal field coils	$N_t = 14$

Table 2 Characteristics of computational model

Equilibrium	Finite-beta Non-circular plasma with given current prifile
Ripple field	Rippled sheet current for TF coils
Initial conditions for alpha particles	According to the local reaction rate by using commulative probability distributions with respect to ψ and poloidal angle
Orbit integration	O(2) Runge-Kutta Guiding-center equation expanded to O(4) in δ Timestep: $\Delta t = 2\pi R_0/20N_t v_{\|\|}$ minimum $v_{\|\|} \sim 0.15v$
Time scale enhancement	No enhancement for banana and some transit particles near banana region 200 for transit particles
Particle loss	Collision with the first wall Local Larmor radius effect
Collisions	Trubinikov operator Random gyrophase slowing down pitch angle scattering speed diffusion no electric field term

Figure captions

Fig. 1 Geometry of plasma and first wall, contours of constant TF ripple.

Fig. 2 Distributions of TF ripple and toroidal flux function ψ in the midplane.

Fig. 3 Safety factor q as a function of toroidal flux function ψ.

Fig. 4 Evolution of time-integrated total power-loss fraction during slowing-down(solid). Dotted curve (red region) shows power-loss fraction of ripple-trapped loss. Difference between solid and dotted curves (blue region) gives power-loss fraction of ripple-enhanced banana-drift loss.

Fig. 5 Evolution of time-integrated total particle-loss fraction during slowing-down(solid). Dotted curve (red region) shows particle-loss fraction of ripple-trapped loss. Difference between solid and dotted curves (blue region) gives particle-loss fraction of ripple-enhanced banana-drift loss.

Fig. 6 Ripple-enhanced banana-drift loss spectrum (blue poles) and ripple-trapped loss spectrum (red poles).

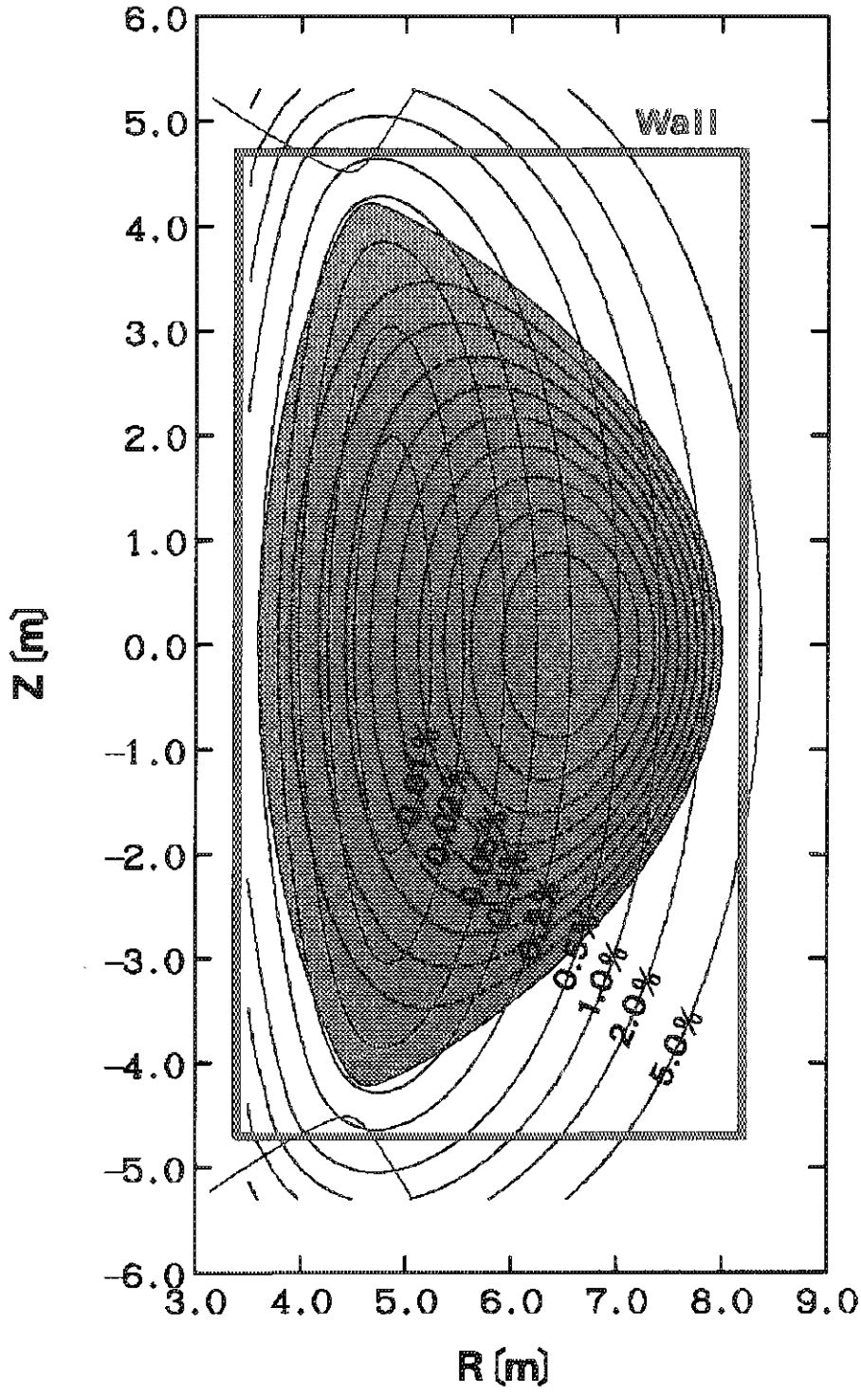
Wall
6.0
5.0
4.0
3.0
2.0
1.0
0.0
-1.0
-2.0
-3.0
-4.0
-5.0
-6.0
3.0
4.0
5.0
6.0
7.0
8.0
9.0
Z (m)
R (m)
0.5%
1.0%
2.0%
5.0%

Fig.1

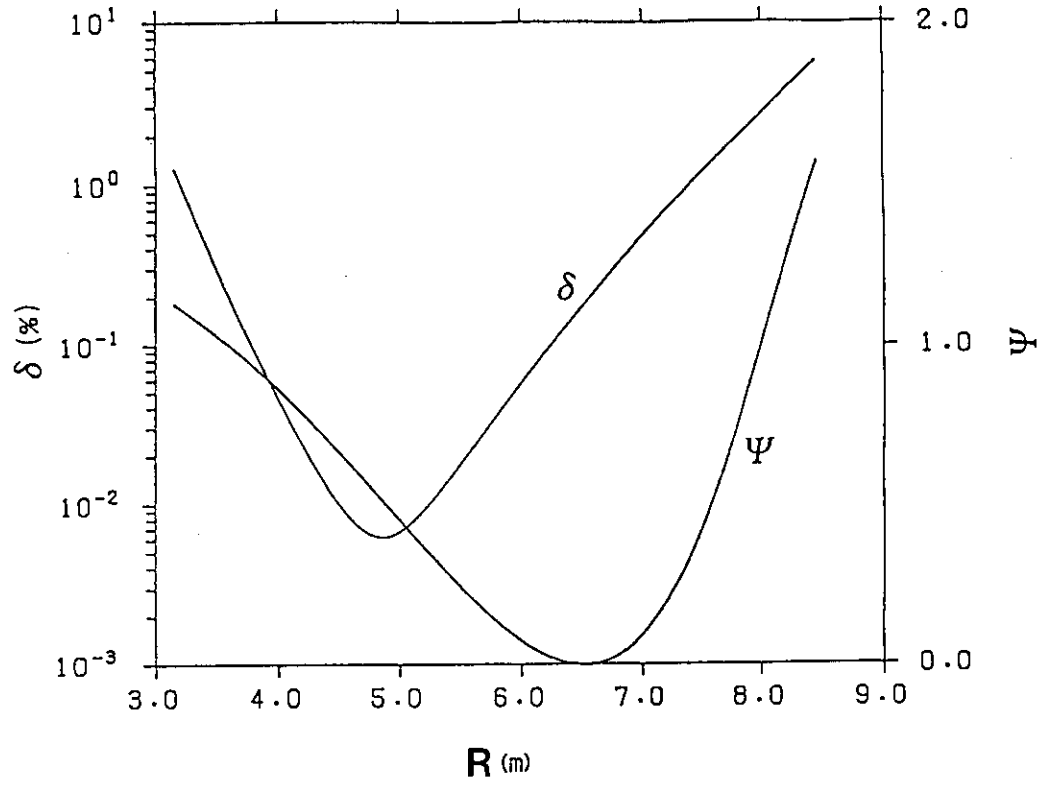
10^1
10^0
10^{-1}
10^{-2}
10^{-3}
δ (%)
2.0
1.0
0.0
Ψ
δ
Ψ
3.0
4.0
5.0
6.0
7.0
8.0
9.0
R (m)

Fig.2

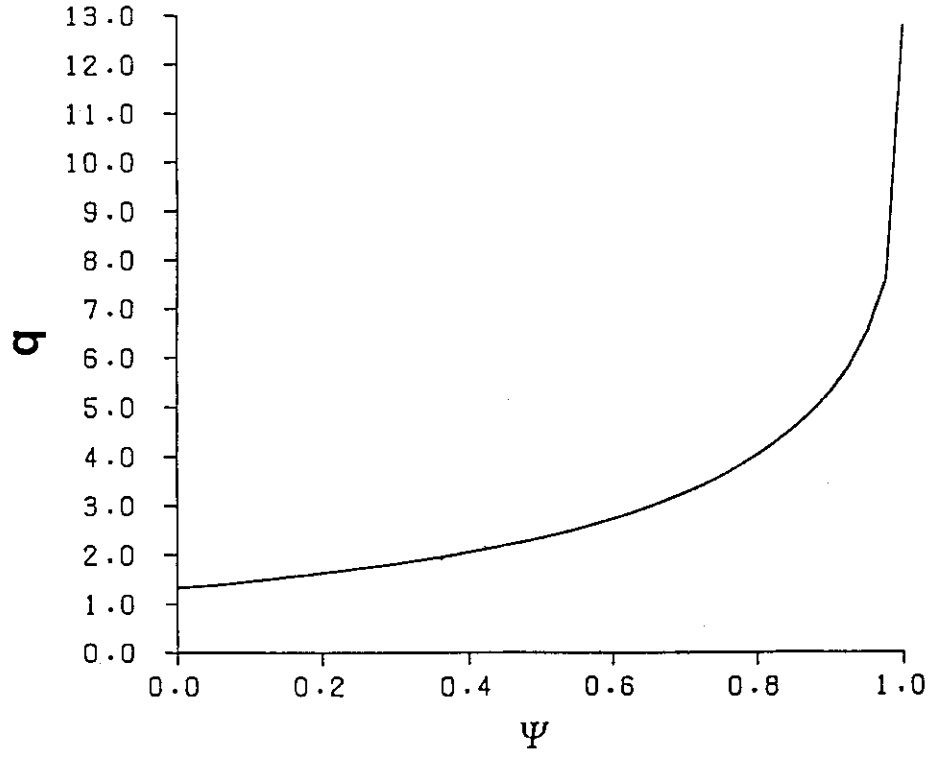
13.0
12.0
11.0
10.0
9.0
8.0
7.0
6.0
5.0
4.0
3.0
2.0
1.0
0.0
q
0.0
0.2
0.4
0.6
0.8
1.0
Ψ

Fig.3

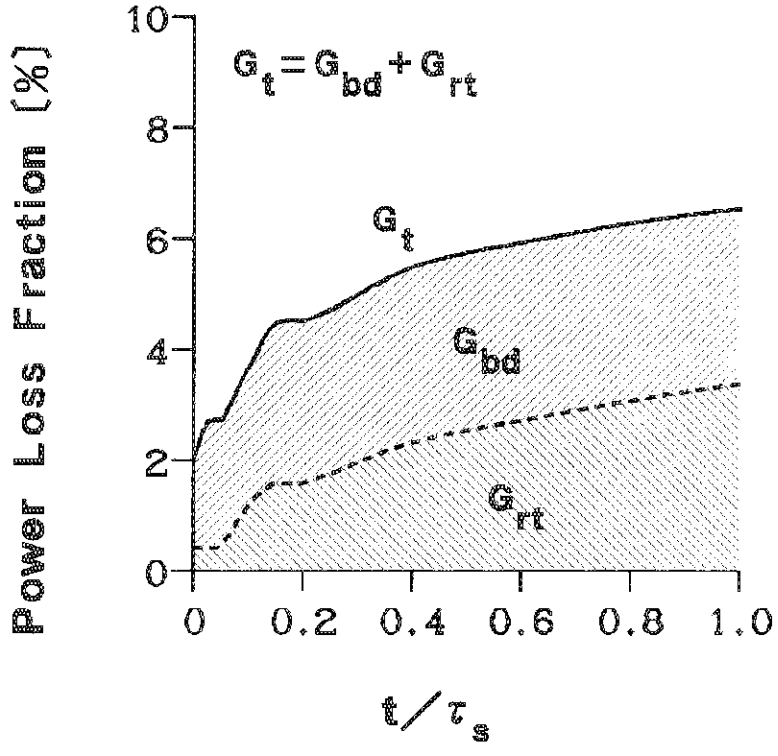
Power Loss Fraction (%)
$G_t = G_{bd} + G_{rt}$
G_t
G_{bd}
G_{rt}
0
2
4
6
8
10
0
0.2
0.4
0.6
0.8
1.0
t/τ_s

Fig.4

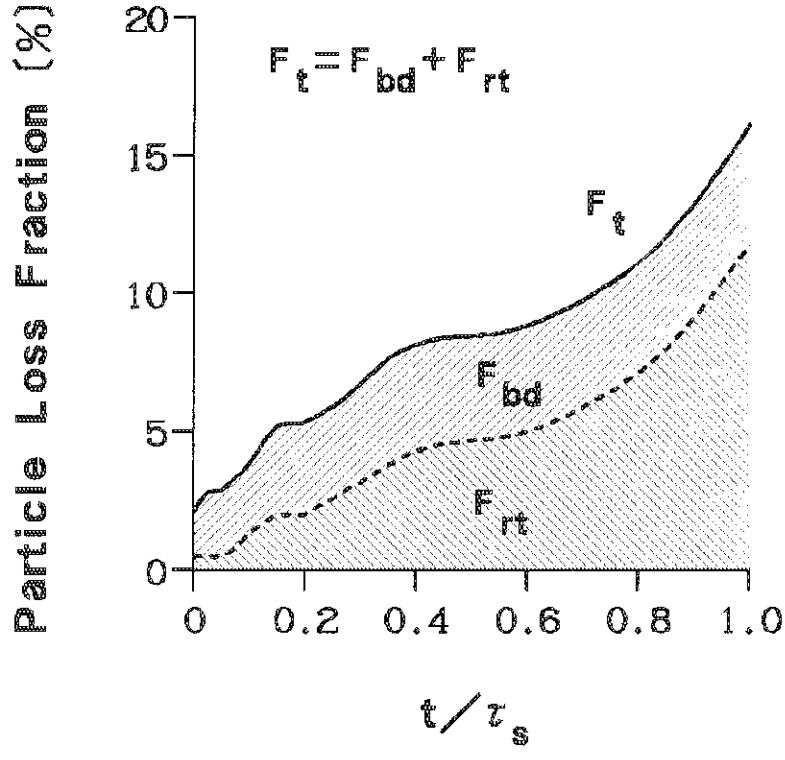
Particle Loss Fraction (%)
$F_t = F_{bd} + F_{rt}$
F_t
F_{bd}
F_{rt}
0
5
10
15
20
0
0.2
0.4
0.6
0.8
1.0
t/τ_s

Fig.5

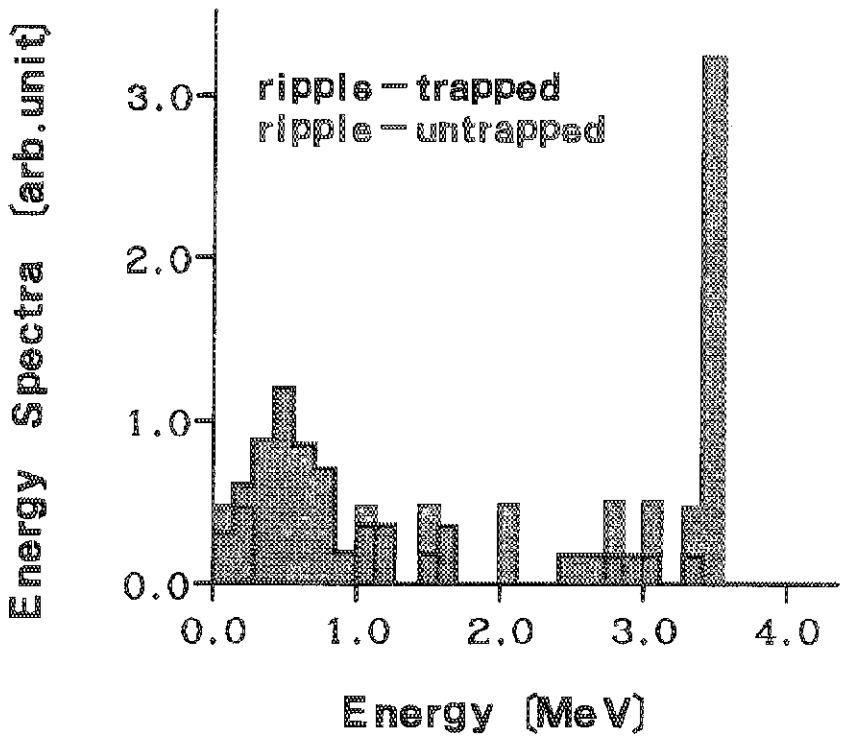
Energy Spectra (arb.unit)
3.0
2.0
1.0
0.0
ripple – trapped
ripple – untrapped
0.0
1.0
2.0
3.0
4.0
Energy (MeV)

Fig.6

II. Heat Load on the First Wall due to Ripple Loss of Alpha Particles in ITER

1. Introduction

Ripple-induced loss of suprathermal alpha particles has a very strong impact not only on the specification of toroidal field coils but also on the design of plasma-facing components such as the first wall and divertor plates. Especially, the peak heat load on the first wall and the divertor plates is one of the critical issues of the design of ITER. Accordingly, we have investigated the two-dimensional heat load by using an orbit-following Monte-Carlo code.

2. Calculation parameters

Calculation has been made for parameters appropriate to ITER design phase-I which are summarized in Table 1. Geometry of MHD equilibrium and constant contours of field ripple are shown in Fig.1. The field ripples at the outer and inner edge of the plasma are 1.5% and 0.06%, respectively. In the present calculation, we employ a realistic first wall shape which is also shown in Fig.1. The wall mesh points used in the calculation are listed in Table 2. The effect of local finite Larmor radius is also taken into consideration. The safety factor q is shown in Fig.2 as a function of ψ(toroidal flux function).

3. Calculation results

In order to save the computational time, test particles are generated only in the region $0.5 < \psi < 1.0$ ($\psi = 0$ on the magnetic axis and 1.0 at the edge). About 3000 test particles are used for one calculation case, and 12 cases of computations have been executed with different random numbers. Through the series of calculations, about 250 loss particles have been accumulated.

For parameters of ITER summarized in Table I, numerically derived power loss fractions for ripple-untrapped loss and ripple-trapped loss are only 0.53% and 0.12%, respectively, and the corresponding particle loss fractions are 0.56% and 0.32%.

Distributions of the heat load averaged over the toroidal angle, hereafter simply referred to as TAA heat load, are shown in Fig.3. The solid and dotted lines show the heat load by ripple-untrapped loss particles and by ripple-trapped loss particles, respectively. The heat loads near

wall-mesh number 40 and 50 are deposited to the divertor plates. The level of the TAA heat load by ripple-trapped loss particles (dotted line) is very low. For the reason mentioned later, the heat load of this kind should not be averaged over the toroidal angle.

Finally, 2-dimensional heat load on the first wall is diagnosed with those 250 loss particles. There is a significant difference between the 2-D distribution of heat load by ripple-trapped loss and that by ripple-untrapped loss [1]. Figure 4 shows the 2-D heat load for ripple-trapped loss particles. Those loss particles are strongly localized. The peak heat load however, is only of the order of 0.1 MW/m^2 because of the very small loss fraction. This level of heat load is low enough for the design of the first wall. The 2-D distribution of heat load for ripple-untrapped loss particles is shown in Fig.5. Due to the low density of loss test particles, the Monte-Carlo error bar seems to be very high. In spite of the Monte-Carlo noise, the toroidal-angle localization seems to be very weak. The toroidal-angle localization mainly comes from the corrugation of the magnetic field line near the first wall. ITER employs the field ripple which is low enough to prevent the toroidal-angle localization of ripple-untrapped loss particles. Consequently, it can be considered that the peak heat load by ripple-untrapped loss is approximately given by the TAA heat load shown in Fig.3. In the present case, the peak heat load is about 0.07 MW/m^2 which is smaller than that by the ripple-trapped loss.

4. Conclusions

Two dimensional heat load on the first wall due to ripple loss of alpha particles in ITER has been estimated by using an orbit-following Monte-Carlo code. Conclusions of the present investigation are summarized as follows:

1) Ripple-trapped loss particles are strongly localized. The peak heat load, however, is only of the order of 0.1 MW/m^2 due to the very small loss fraction.
2) The toroidal-angle localization of ripple-untrapped loss particles seems to be very weak in ITER. The peak heat load averaged over the toroidal angle is about 0.07 MW/m^2.

Reference

[1] TANI, K., KISHIMOTO, H., Nucl. Fusion 22 (1982) 1108.

Table 1 Calculation parameters

major radius	$R_t = 5.8\ m$
minor radius	$a = 2.2\ m$
toroidal field	$B_t = 4.4\ T$
plasma temperature	$T_e(\Psi) = T_{e0}(1-\Psi)$
	$T_i(\Psi) = T_{i0}(1-\Psi)$
	$T_D(\Psi) = T_T(\Psi) = T_i(\Psi)$
	$T_{e0} = T_{i0} = 20\ keV$
plasma density	$n_e(\Psi) = n_{e0}(1-\Psi)^{0.5}$
	$n_D(\Psi) = n_T(\Psi) = n_i(\Psi)$
	$n_{e0} = 2.0 \times 10^{20}\ m^{-3}$
plasma current	$j(\Psi) = j_0(1-\Psi)^{0.5}$
	$I_p = 22\ MA$
ellipticity	$\kappa = 1.96$
triangularity	$\Delta = 0.55$
effective Z	$Z_{eff} = 1.5$ (uniform)
charge number of impurity ion	$Z_{imp} = 8.0$ (oxygen)
number of toroidal field coils	$N_t = 16$

Table 2 Wall surface mesh points

WALL SURFACE MESH (R,Z) m

	1		2		3		4		5		6		7		8		9		10	
0	3.45	0.0	3.45	0.13	3.45	0.26	3.45	0.39	3.46	0.52	3.46	0.65	3.47	0.78	3.47	0.91	3.48	1.04	3.49	1.17
1	3.49	1.30	3.50	1.43	3.51	1.56	3.52	1.69	3.54	1.82	3.55	1.95	3.56	2.08	3.58	2.21	3.59	2.34	3.61	2.47
2	3.62	2.60	3.64	2.73	3.66	2.86	3.68	2.99	3.70	3.12	3.72	3.25	3.75	3.37	3.77	3.50	3.79	3.63	3.92	3.63
3	4.04	3.63	4.07	3.75	4.09	3.88	4.11	4.00	4.13	4.13	4.16	4.25	4.18	4.38	4.20	4.50	4.23	4.63	4.25	4.75
4	4.36	4.82	4.47	4.89	4.57	4.96	4.68	5.03	4.79	5.10	4.90	5.17	5.01	5.25	5.12	5.32	5.22	5.39	5.33	5.46
5	5.44	5.53	5.55	5.60	5.66	5.60	5.77	5.60	5.89	5.60	6.00	5.60	6.00	5.47	6.00	5.35	6.00	5.22	6.00	5.10
6	6.00	4.97	6.00	4.85	6.00	4.72	6.00	4.60	6.10	4.51	6.20	4.42	6.30	4.33	6.39	4.24	6.48	4.15	6.58	4.05
7	6.66	3.95	6.75	3.85	6.83	3.75	6.92	3.64	7.00	3.54	7.07	3.43	7.15	3.32	7.22	3.21	7.29	3.09	7.36	2.98
8	7.42	2.86	7.48	2.75	7.54	2.63	7.60	2.51	7.65	2.39	7.71	2.26	7.75	2.14	7.80	2.02	7.84	1.89	7.88	1.77
9	7.92	1.64	7.96	1.51	7.99	1.38	8.02	1.25	8.04	1.12	8.07	0.99	8.09	0.86	8.11	0.73	8.12	0.60	8.13	0.46
10	8.14	0.33	8.15	0.20	8.15	0.07	8.15	-0.07	8.15	-0.20	8.14	-0.33	8.13	-0.46	8.12	-0.60	8.11	-0.73	8.09	-0.86
11	8.07	-0.99	8.04	-1.12	8.02	-1.25	7.99	-1.38	7.96	-1.51	7.92	-1.64	7.88	-1.77	7.84	-1.89	7.80	-2.02	7.75	-2.14
12	7.71	-2.26	7.65	-2.39	7.60	-2.51	7.54	-2.63	7.48	-2.75	7.42	-2.86	7.36	-2.98	7.29	-3.09	7.22	-3.21	7.15	-3.32
13	7.07	-3.43	7.00	-3.54	6.92	-3.64	6.83	-3.75	6.75	-3.85	6.66	-3.95	6.58	-4.05	6.48	-4.15	6.39	-4.24	6.30	-4.33
14	6.20	-4.42	6.10	-4.51	6.00	-4.60	6.00	-4.72	6.00	-4.85	6.00	-4.97	6.00	-5.10	6.00	-5.22	6.00	-5.35	6.00	-5.47
15	6.00	-5.60	5.89	-5.60	5.77	-5.60	5.66	-5.60	5.55	-5.60	5.44	-5.53	5.33	-5.46	5.22	-5.39	5.12	-5.32	5.01	-5.25
16	4.90	-5.17	4.79	-5.10	4.68	-5.03	4.57	-4.96	4.47	-4.89	4.36	-4.82	4.25	-4.75	4.23	-4.63	4.20	-4.50	4.18	-4.38
17	4.16	-4.25	4.13	-4.13	4.11	-4.00	4.09	-3.88	4.07	-3.75	4.04	-3.63	3.92	-3.63	3.79	-3.63	3.77	-3.50	3.75	-3.37
18	3.72	-3.25	3.70	-3.12	3.68	-2.99	3.66	-2.86	3.64	-2.73	3.62	-2.60	3.61	-2.47	3.59	-2.34	3.58	-2.21	3.56	-2.08
19	3.55	-1.95	3.54	-1.82	3.52	-1.69	3.51	-1.56	3.50	-1.43	3.49	-1.30	3.49	-1.17	3.48	-1.04	3.47	-0.91	3.47	-0.78
20	3.46	-0.65	3.46	-0.52	3.45	-0.39	3.45	-0.26	3.45	-0.13										

Figure captions

Fig. 1 Geometry of plasma and first wall, contours of constant TF ripple.

Fig. 2 Safety factor q as a function of toroidal flux function ψ.

Fig. 3 Distributions of heat load averaged over toroidal angle for ripple-untrapped (solid) and ripple-trapped (dotted) loss particles.

Fig. 4 Two-dimensional heat load on the first wall for ripple-trapped loss particles

Fig. 5 Two-dimensional heat load on the first wall for ripple-untrapped loss particles

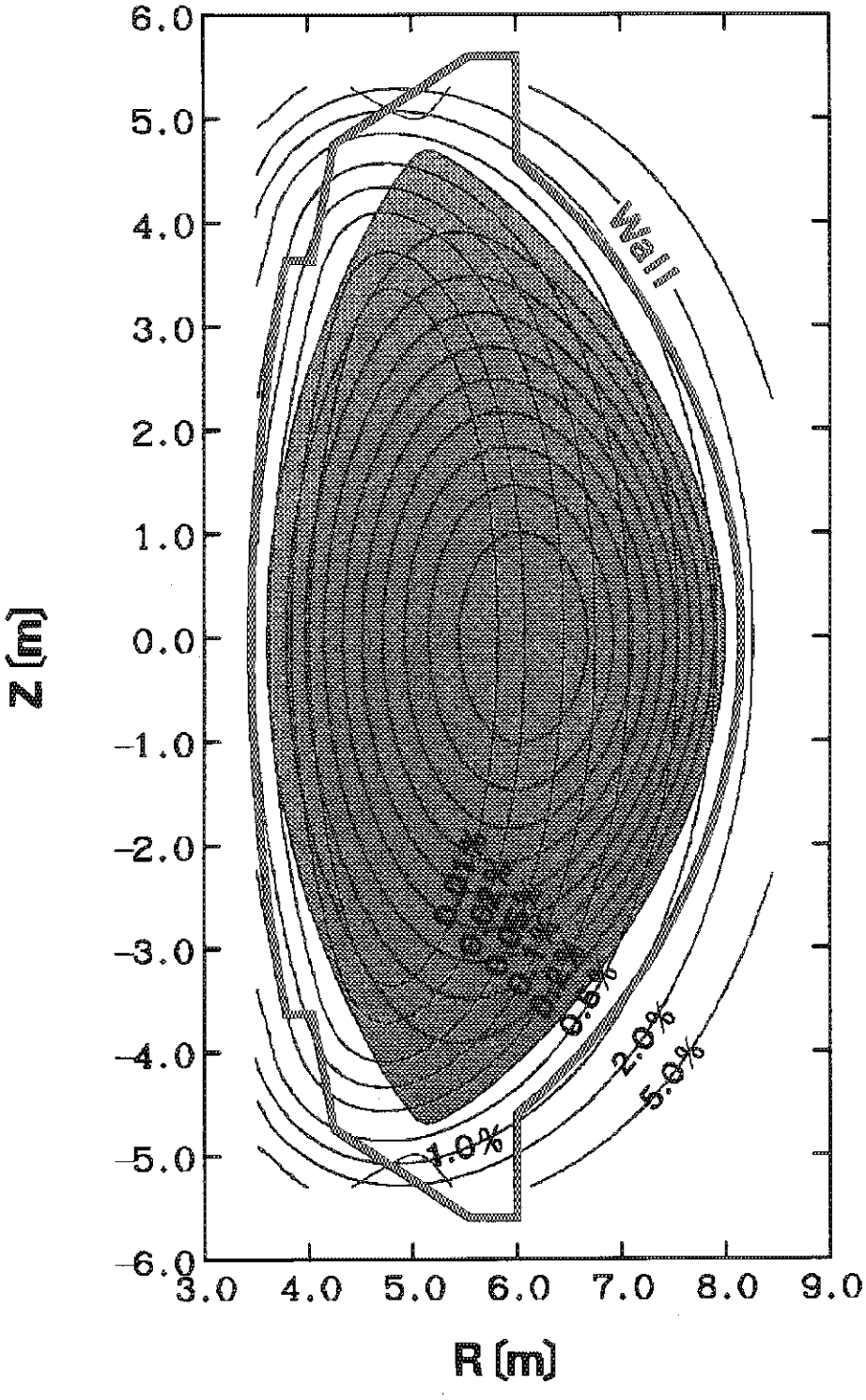
6.0
5.0
4.0
3.0
2.0
1.0
0.0
-1.0
-2.0
-3.0
-4.0
-5.0
-6.0
Z (m)
3.0
4.0
5.0
6.0
7.0
8.0
9.0
R (m)
Wall
0.5%
2.0%
5.0%
1.0%

Fig.1

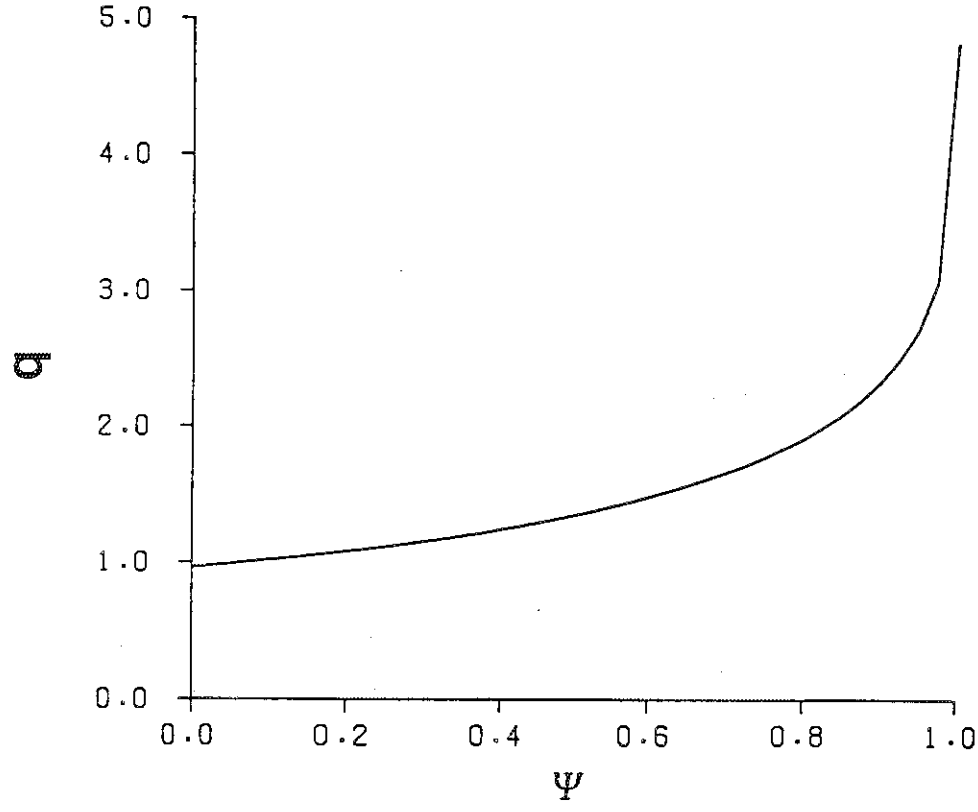

Fig.2

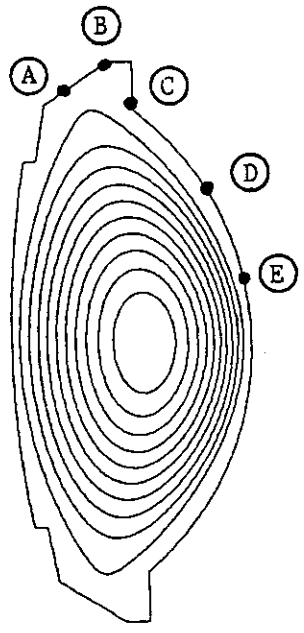
B
A
C
D
E

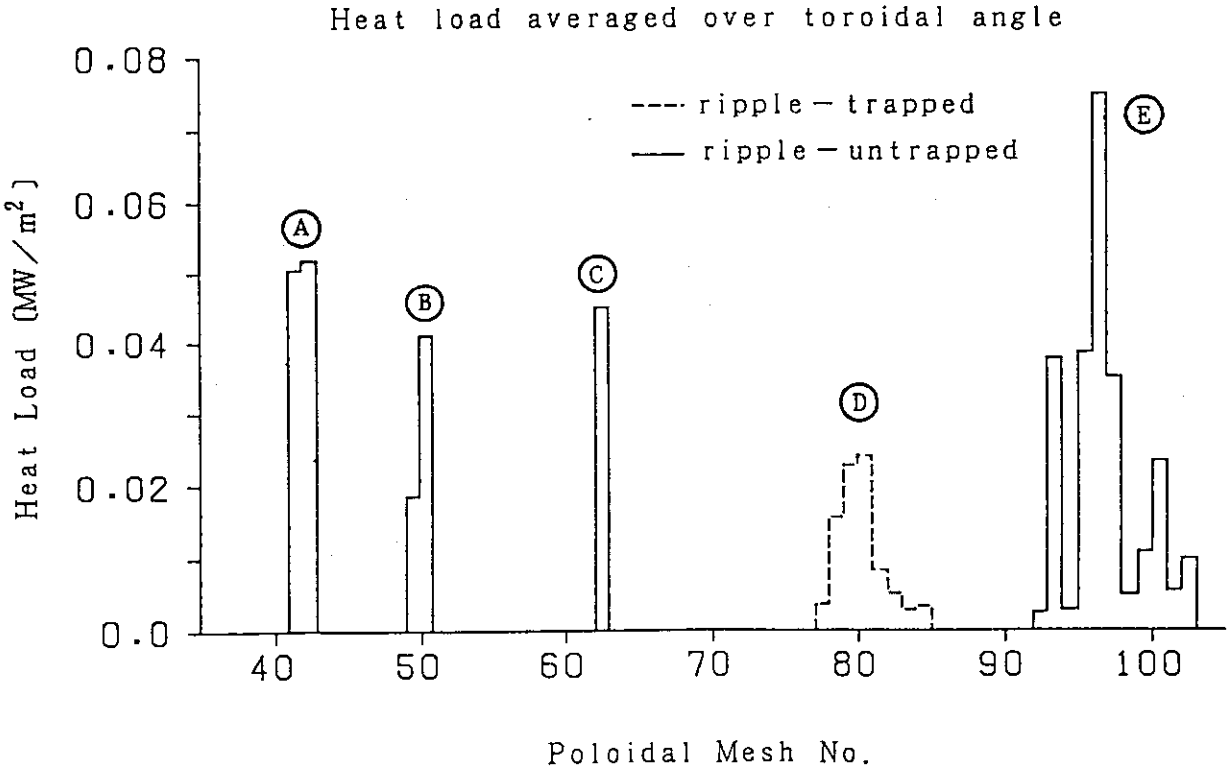
Heat load averaged over toroidal angle
---- ripple－trapped
—— ripple－untrapped
Heat Load (MW/m²)
0.08
0.06
0.04
0.02
0.0
40
50
60
70
80
90
100
Poloidal Mesh No.

Fig.3

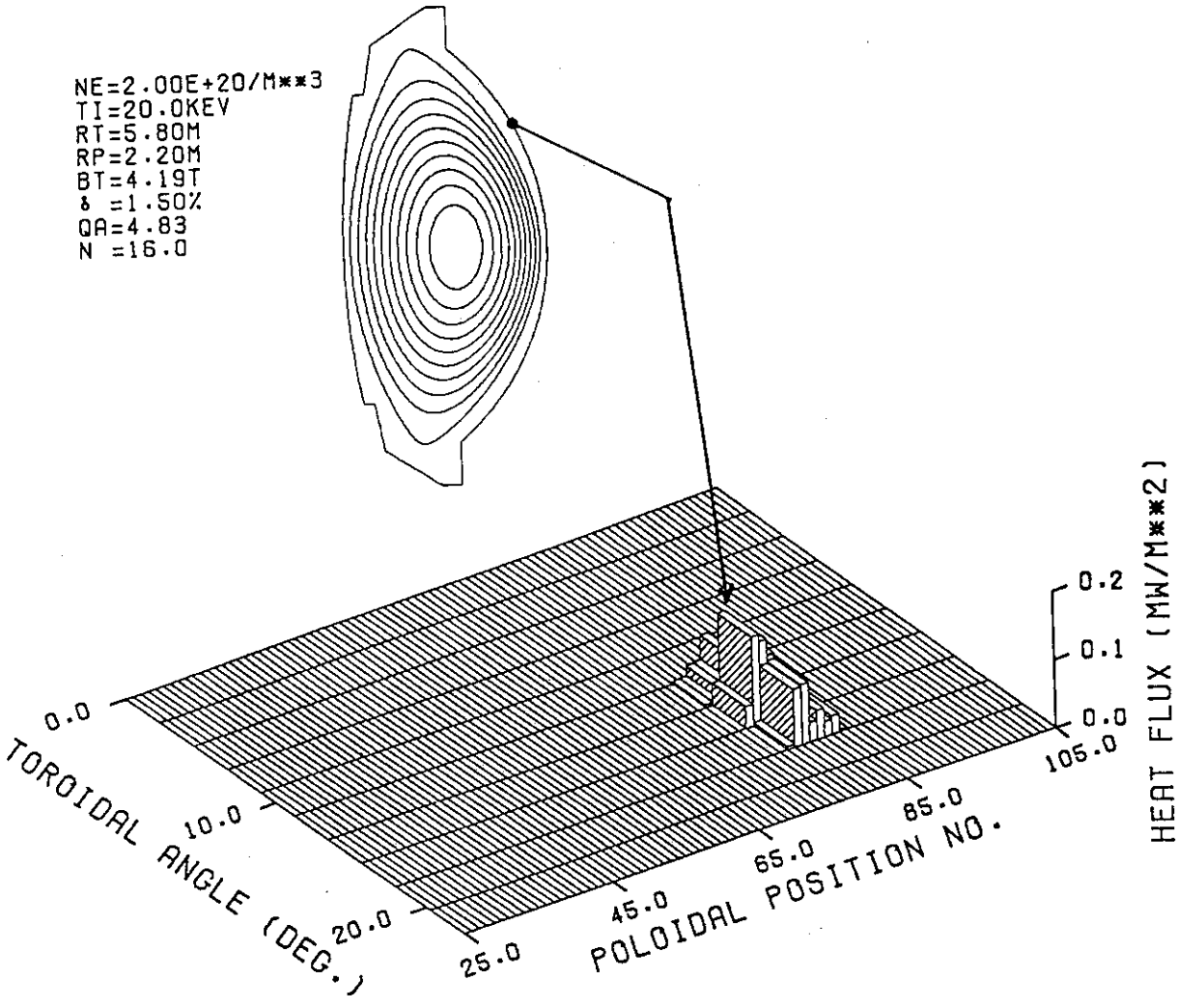
NE=2.00E+20/M**3
TI=20.0KEV
RT=5.80M
RP=2.20M
BT=4.19T
δ =1.50%
QA=4.83
N =16.0
0.0
10.0
20.0
TOROIDAL ANGLE (DEG.)
25.0
45.0
65.0
85.0
105.0
POLOIDAL POSITION NO.
0.0
0.1
0.2
HEAT FLUX (MW/M**2)

Fig.4

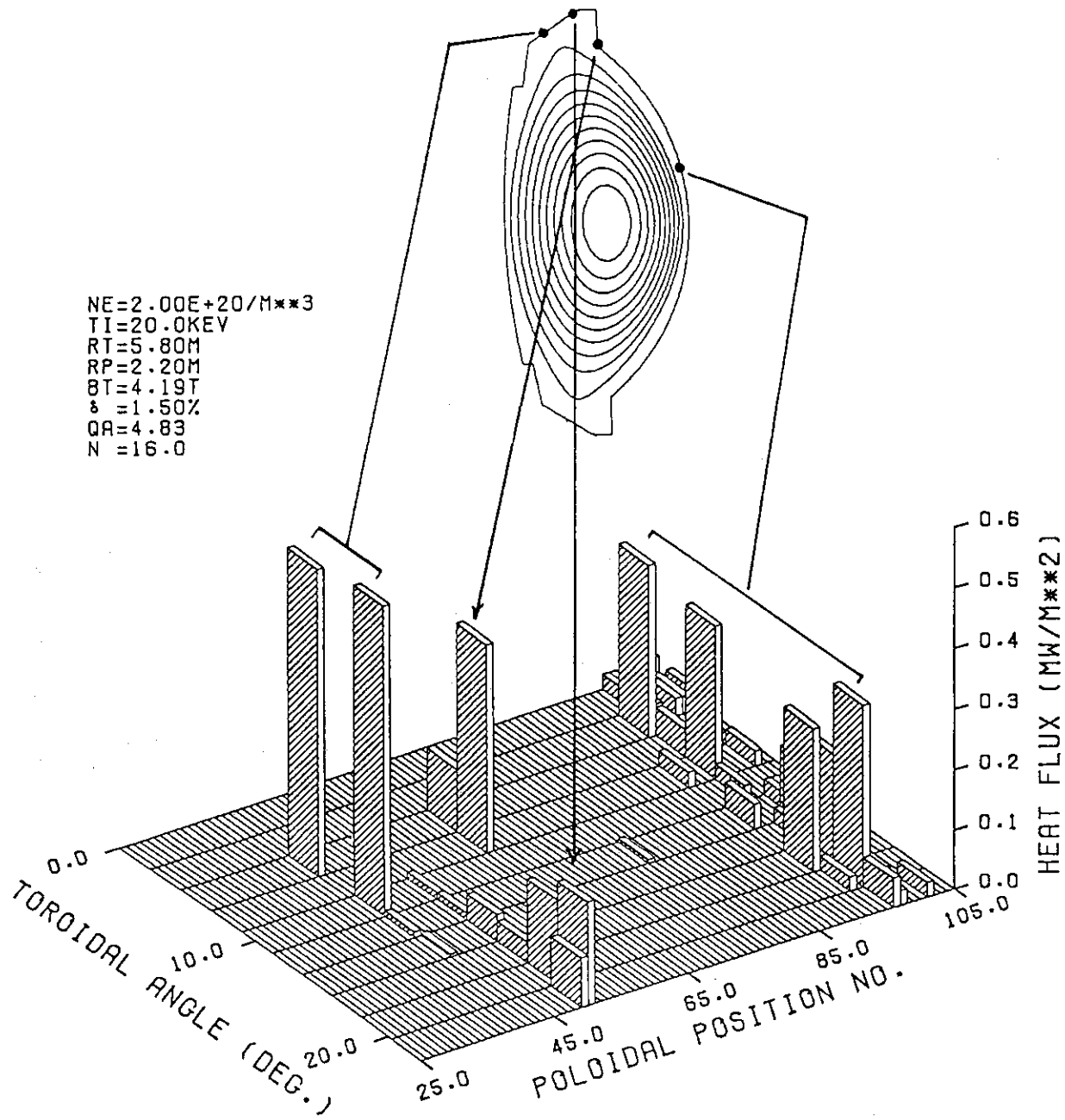
NE=2.00E+20/M**3
TI=20.0KEV
RT=5.80M
RP=2.20M
BT=4.19T
β =1.50%
QA=4.83
N =16.0
0.0
10.0
20.0
TOROIDAL ANGLE (DEG.)
25.0
45.0
65.0
85.0
105.0
POLOIDAL POSITION NO.
0.0
0.1
0.2
0.3
0.4
0.5
0.6
HEAT FLUX (MW/M**2)

Fig.5